



Comparing conventional manual measurement of the green view index with modern automatic methods using Google Street View and semantic segmentation



Tetsuya Aikoh^{a,*}, Riko Homma^b, Yoshiki Abe^c

^a Research Faculty of Agriculture, Hokkaido University, Japan

^b ai Landscape Planning Co., Ltd, Japan

^c Softcomm Co., Ltd, Japan

ARTICLE INFO

Keywords:

Green view index
Google Street Map
Semantic segmentation
Urban green space

ABSTRACT

Urban greenery has various beneficial effects, such as engendering peace of mind. The green view index (GVI) effectively measures the amount of greenery people can perceive and is a suitable indicator of urban greening. To date, the most common way to measure the GVI has been to photograph the street environment from eye level and use image-editing software to calculate the area occupied by vegetation. However, conventional methods are time-consuming and labor-intensive, and the calculation results may vary among individuals. In recent years, the use of Google Street View (GSV) photos and calculation of the GVI using automatic image segmentation have rapidly developed. In this study, we demonstrate the advantages of GSV and image segmentation over conventional methods, verify their accuracy, and identify the shortcomings of modern methods. We calculated the GVI in the central part of Sapporo, Japan, using the automatic image segmentation AI "DeepLab" and compared the results with those measured by Photoshop. At the exact GSV locations, we also acquired photos and again calculated the GVI using AI, subsequently comparing the results with those obtained on-site manually. Although the correlations were high, automatic image segmentation tended not to identify lawns and flowers planted in the ground as vegetation. It was impossible to determine the year when the GSV photos were taken. In addition, the distance to greenery was biased, depending on the position on the street. These points should be considered when using these modern methods.

1. Introduction

1.1. Benefits of green view

Urban green spaces, such as parks, street trees, shrubs, lawns, and flower beds, are essential elements of the urban landscape (Schroeder and Cannon, 1983; Thayer and Atwood, 1978; Wolf, 2005). They provide a variety of benefits to urban environments. For example, they absorb carbon dioxide (Nowak and Crane, 2002), remove air pollutants (Jim and Chen, 2008), reduce stormwater runoff (Liu et al., 2014; Zhang et al., 2012), mitigate urban heat islands (Chen et al., 2006; Onishi et al., 2010), supply urban ecosystem services (Derkzen et al., 2015). In addition, green spaces promote health and well-being (Douglas et al., 2017), fulfill the psychological, social, and cultural needs of urban residents (Dwyer et al., 1991), relate the social capital (Holtan et al., 2015),

bring psychological benefits (Buxton et al., 2019; Lee and Maheswaran, 2011; Leslie et al., 2010; Tyrväinen et al., 2014), and decrease crime rate (Troy et al., 2012).

To understand the amount of urban green space and evaluate its effectiveness, the most commonly used method is the "green cover ratio," which is the area of parks or the ratio of green space or the tree canopy cover to a certain amount of land. The green cover ratio is estimated by manually measuring the extracted vegetated area from satellite images or aerial photographs by extracting vegetation from color bands using infrared aerial photographs or by using satellite photographs to calculate the normalized difference vegetation index (NDVI; Dymond et al., 1992; Gupta et al., 2012). The amount of green areas shown by the NDVI and the amount of tree canopy cover contribute to improving mental health. (Beyer et al., 2014, Browning et al., 2019, Cohen-Cline et al., 2015). However, several studies have

* Correspondence to: Research Faculty of Agriculture, Hokkaido University, Kita9, Nishi9, Kita-ku, Sapporo, Hokkaido 060-8589, Japan.

E-mail addresses: tetsu@res.agr.hokudai.ac.jp (T. Aikoh), rikohomma@gmail.com (R. Homma), happy.trail0912@gmail.com (Y. Abe).

shown that the amount of greenery identified from the sky, such as aerial photographs and satellite images, differs from the amount and type of greenery identified via photographs taken at the eye level of the people (Yang et al., 2009; Ye et al., 2019a). Kumakoshi et al. (2020) stated that it is desirable to use NDVI for parks and forests, and visibility of greenery at street level for city centers.

In contrast, the “green view index (GVI)” has been attracting attention in recent years. The GVI is the percentage of vegetated areas in the field of vision; this metric may better represent people’s perception of greenery (Aoki, 1991). It also captures greenery that cannot be measured by the green cover ratio, such as wall greening, shrubs growing under trees, and street flowers. Schroeder and Cannon (1983) found that the area of vegetation in the street environment affects people’s perceptions of the desirability of that location. Visible vegetation and trees influence landscape preference (Jiang et al., 2015) and enhance the attractiveness of the recreational setting (Bjerke et al., 2006). They also influence people’s perceptions of safety and naturalness (Suppakittpaisarn et al., 2020), reduce stress (Jiang et al., 2014; Jiang et al., 2016; Elsadek et al., 2019), and improve mental health during the COVID-19 pandemic (Soga et al., 2021). The greenery of the neighborhood also affects land prices (Gao and Asami, 2007), and the rent of commercial buildings (J. Yang et al., 2021).

Yang et al. (2009) defined the concept of urban green visibility as the GVI and examined the correlations between the GVI and green cover ratio. It has also been confirmed that the GVI is closer to the amount of greenery perceived by people than green coverage (Falfán et al., 2018; Jiang et al., 2017; Leslie et al., 2010). Associations between the GVI and physical activities were examined, such as the duration of walking, jogging, and cycling (Lu, 2019), walking time (Lu, 2018; Lu et al., 2018; Yang et al., 2019; L. Yang et al., 2021), number of visitors in parks (Y. Yang et al., 2021), walkability (Yin and Wang, 2016; Zhou et al., 2019; Nagata et al., 2020). And between the GVI and both residents’ socio-economic status and housing prices (Li et al., 2015b; Ye et al., 2019b).

The green view index is a necessary indicator for considering the supply and arrangement of urban green spaces. For example, Japanese local authorities have formulated green basic plans, which define policies for the supply and maintenance of urban parks, conservation of urban green space, and greening in urban areas. The plans are required to include quantitative indicators. The green coverage ratio has been used as an indicator by most local authorities. Recently, an increasing number of local authorities have set targets for the GVI as an indicator in their plans, in addition to the green coverage ratio (Tonosaki, 2010). A manual published by the Osaka Prefecture in 2013 has been commonly used. However, there is the issue of the time and cost involved in taking photographs and calculating the greenness ratio. Planners and practitioners want more efficient methods.

1.2. Collection of photographs

In contrast to the conventional method of collecting photographs of street greenery from the human eye level, there is increasing interest in using online street view photographs. This is because surveying and photographing green spaces and trees in the field is time-consuming, costly, and subject to safety risks and weather and seasonal conditions (Berland and Lange, 2017; Lu, 2019). The photographs in Google Street View (GSV) were predominately captured by cameras mounted on the roofs of cars on the roadway. The camera height was 2.45 m, but the camera height was gradually lowered to 2.05 m to match the width of the road and the housing conditions in Japan. GSV covers streets in cities and suburbs worldwide; in some cases, photos were taken from indoors, underground passages, and parkways. Google has also released the Google Street View API, a mechanism for sharing software functions. The Google Street View Image API makes it possible to obtain any GSV photograph on the web by setting the following five parameters: latitude and longitude of the point, direction, horizontal field of view angle, camera angle, and output image size. In other research areas, GSV has

been used to evaluate neighborhood environments (Berland and Lange, 2017; Griew et al., 2013; Odgers et al., 2012; Rundle et al., 2011; Xia et al., 2021; Yin & Wang, 2016). Google is not alone in these efforts. In China, studies have been conducted using photos from Tencent (Dong et al., 2018; Liu et al., 2021; Long and Liu, 2017; Zhang and Dong, 2018), which provides a similar service, and Baidu (Chen et al., 2019; Chen et al., 2020; Wu et al., 2020; Xiao et al., 2021; Ye et al., 2019b). These services can reduce the time, labor, cost, safety risk and constraint of weather conditions of an on-site survey (Berland and Lange, 2017; Lu et al., 2018; Lu, 2019; Ye et al., 2019a).

On the other hand, Xia et al. (2021) noted that GSV photos are not the same as the actual view experienced by pedestrians. The GSV is taken from the center of the road, which is somewhat different from the field of view of a pedestrian. Regarding the field of view, some studies set the horizontal angle of GSV to 60 degrees, considering the human field of view (Li et al., 2015a), referring to the past study by Yang et al. (2009). Because GSV can obtain pictures from various angles, Li et al. (2015b) obtained 18 photos at one location, six horizontal and three verticals, to calculate GVI; Dong et al. (2018) set the angle of view to 72 degrees and used photos from six orientations. The most common examples calculate the green view index for a 360-degree range from four photos with a 90-degree angle of view (Lu et al., 2018; Lu, 2019; Yang et al., 2019; Labib et al., 2021; J. Yang et al., 2021). Some studies use panoramic photographs (Gong et al., 2018; Chen et al., 2019).

Other studies have also pointed out problems such as the limited season and time when the photos are taken (Gong et al., 2018; Ki and Lee, 2021; Li et al., 2015a; Li et al., 2017; Lu, 2019; Nagata et al., 2020; Xia et al., 2021; Yang et al., 2019; Ye et al., 2019a), the fact that the photos are mainly taken from the roadway (Li et al., 2015a; Wu et al., 2020), and the fact that objects on the sidewalk may be hidden by cars or other objects between the camera on the car and the sidewalk (Lu, 2019; Rundle et al., 2011; Yang et al., 2019). Although the possibility of these GSV weaknesses has been known, there has been no concrete verification.

1.3. Measurement of Green View Index (GVI)

To calculate the GVI, From the 1970s to the 1990s, the gravimetric method was used, which separates the vegetation and other parts shown in a photograph and weights them, and the point grid plate method, which involves placing a point grid transparent plastic sheet on a photograph and counting the number of points included in the vegetated areas (Tonosaki, 2010). Until recently, the mainstream method was to specify the vegetated area in a photograph using image editing software, such as Photoshop, and thereby calculate the GVI (Buxton et al., 2019; Falfán et al., 2018; Jiang et al., 2014; Jiang et al., 2016; Jiang et al., 2017; Labib et al., 2021; Yang et al., 2009). One of the problems with these conventional measurement methods is that they require considerable time and human resources (Chen et al., 2015). The calculation of the GVI has large time and effort demands because all of the methods are manual; further, the results may vary depending on the operator (Tonosaki, 2010).

To improve the efficiency of GVI measurement, a method was introduced that utilizes extraction of color from photographs. This method extracts greenery by selecting vegetation manually or selecting photograph pixels based on tone and color (Yang et al., 2009). The correlation between this method of extracting greenery and the manual method was found to be high ($r = 0.981$; Tonosaki, 2010). However, some issues need to be addressed, such as the fact that the color-based method can misjudge trees on water surfaces, or forests in the distance. Other methods have also been developed to extract vegetation areas based on the difference in reflectance of the three primary colors of light to vegetation (Kumakoshi et al., 2020; Li et al., 2015a; Li et al., 2017; Lu et al., 2018; Lu, 2019; J. Yang et al., 2021). Long and Liu (2017) and others focused on the value of the hue channel from the HSV images (Chen et al., 2020; Dong et al., 2018). Brown Dog Green Index

tool, a web-based service for identifying green vegetation, is also used (Li et al., 2018; Suppakkpaisarn et al., 2019; Suppakkpaisarn et al., 2022). Li et al. (2015a) found that the correlation between the green area extraction and manual measurement using image editing software was 0.96, while Lu et al. (2018) and Lu (2019) found a correlation of 0.91. Dong et al. (2018) found a correlation of 0.971 and Suppakkpaisarn et al. (2022) found a correlation of 0.96.

Subsequently, Lu (2018) used automatic image identification AI to calculate the GVI. This AI uses a deep learning algorithm called “semantic segmentation,” which associates labels or categories such as “sky,” “vegetation,” “building,” and “road” with every pixel in a photograph (Garcia-Garcia et al., 2018; Poursaeed et al., 2018; Seiferling et al., 2017). It has been applied in automated car driving and medical image processing. AI technology is still developing and various

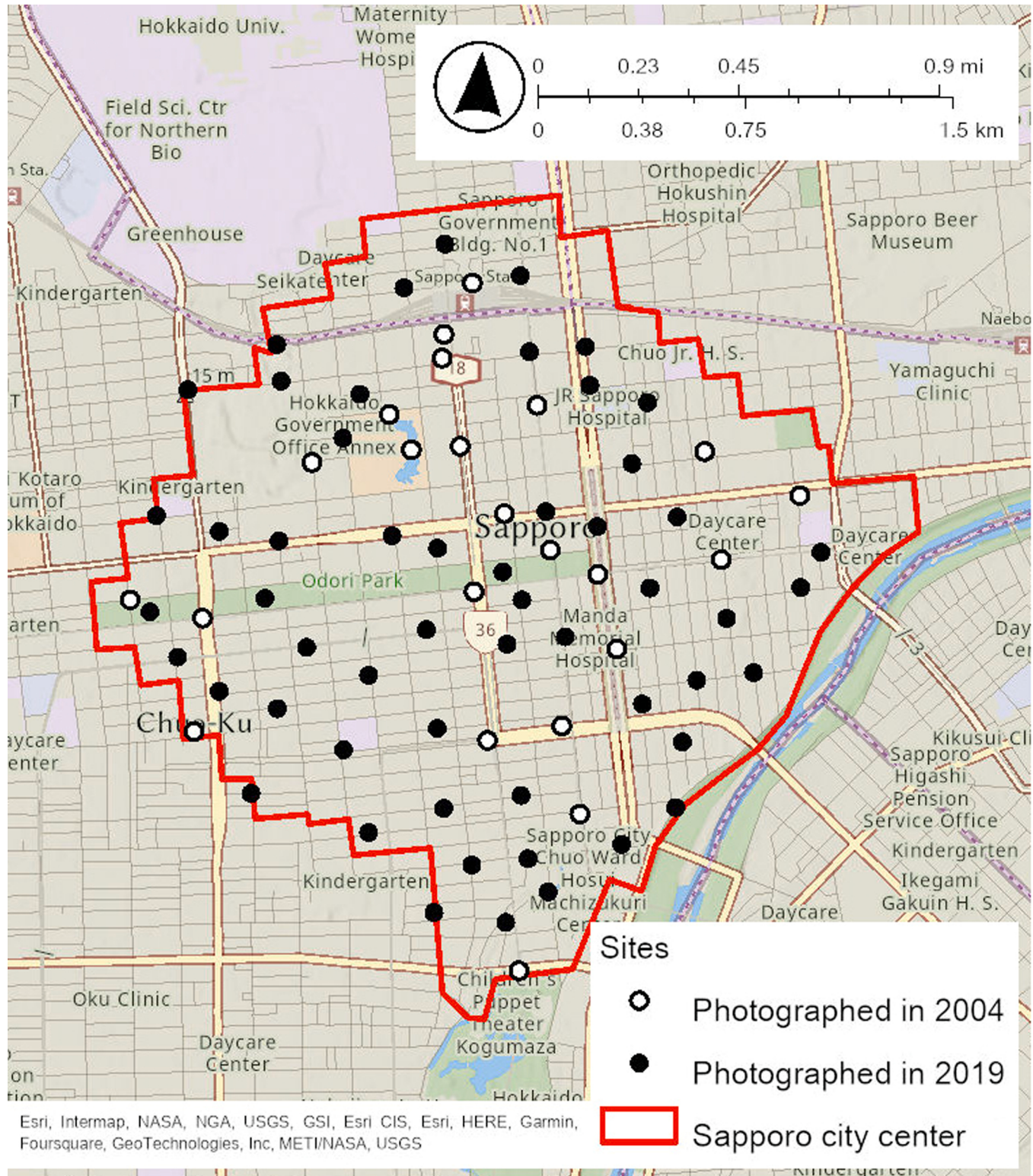


Fig. 1. Research Site and Photograph Locations.

models can be found, but there is no adequate comparison with conventional methods that use image editing software. Examples of automatic image identification AI include PSPNet (Gong et al., 2018; Lu, 2018; Yang et al., 2019, Y. Yang et al., 2021), which has been used in several GVI studies; SegNet (Badrinarayanan et al., 2017; Dong et al., 2018; Ye et al., 2019a, Ye et al., 2019b; Zhou et al., 2019); FCN8s (Ki and Lee, 2021; L. Yang et al., 2021); Back Propagation neural-network (Chen et al., 2019) and DeepLab (Chen et al., 2018; Nagata et al., 2020; Xia et al., 2021). Correlations between greenness calculations by some of these automatic image identification AIs and conventional Photoshop-based manual greenness calculations have been shown, such as $r = 0.91$ for PSPNet (Lu, 2018), $r = 0.899$ (Ye et al., 2019a) or 0.992 (Dong et al., 2018) or 0.98 (Zhang and Dong, 2018) for SegNet, $r = 0.90$ for FCN-8s (L. Yang et al., 2021), and $r = 0.9552$ for DeepLab (Xia et al., 2021). However, color-based greenery extraction and semantic segmentation methods still have the problem of misidentifying green signs, windows, shade, and green artificial objects as vegetation (Chen et al., 2020; Dong et al., 2018; Li et al., 2015a; Long and Liu, 2017; Lu, 2019; Seiferling et al., 2017).

As described above, modern methods have been introduced to measure the GVI in recent years. Such new methods may render it easier to conduct greenness studies efficiently; planners could use these methods to help practitioners develop and improve green spaces so that the spaces better accord with citizens' desired experiences. In contrast, the effectiveness of green ratio measurements using GSV and automatic image identification AI has been confirmed, but the bias against conventional methods needs to be clarified to improve its accuracy and recommend them to practitioners. In this study, we compared the efficiency of conventional methods with the modern methods, using the urban center of Sapporo, Japan, as a test case to verify their efficiency and to identify biases.

2. Methods

2.1. Research site

The city center of Sapporo, Hokkaido, Japan, was chosen as the study site. Sapporo is a city with more than 1.9 million people, and its central area is home to many business and commercial districts. In addition to the 23 locations where the city of Sapporo surveyed the GVI in 2004, 54 new locations were added to the survey so that they would be evenly distributed across the city center. Photographs were taken at these locations (Fig. 1). Various types of roads included intersections, T-junctions, roads with sidewalks, roads without sidewalks, and parks.

2.2. Photographs

To compare the calculation of the green view index between manual and automatic, we collected and took photographs taken in the past: in 2004, Sapporo, Japan, on the sidewalks of 23 intersections, from a height of 150 cm, 1–5 photographs were taken with a 35 mm camera from the corner of the intersection in the direction of the sidewalk. The total number of photographs was 69; photographs were taken at the same locations and directions in 2019. From the end of July to the beginning of August 2019, we took photographs for a total of nine days on bright cloudy or sunny days without rain, avoiding clear days without clouds to avoid backlighting as much as possible. Photographs were captured between 5 a.m. and 9 a.m. to avoid traffic, from a height of 150 cm, which is the distance of the average person's eyes from the ground. The focal distance was adjusted to between 35 mm and 36 mm, a distance that has often been adopted in past surveys using the OLYMPUS TG-835. The angle of the horizontal field of view was approximately 62°, and the photograph aspect ratio was 4:3, 4608 × 3456 pixels (1–4 Mb file size). Thirty-eight photographs from 21 sites with no change in road geometry or surrounding architecture from 2004 were included in the analysis.

Conventional GVI has used photographs taken from the viewpoint of pedestrians on the sidewalk, whereas GSV is taken on the roadway. Therefore, a combination of photographs taken in four directions or panoramic photographs has been used to calculate the green view index (Labib et al., 2021). In this study, a horizontal angle of about 60 degrees, which is close to the human visual field, was employed (Li et al., 2015a). In addition, following Osaka Prefecture's guidelines for green view index surveys (Osaka Prefecture, 2013), the green view index of multiple fields of vision of pedestrians was calculated at a single location, and the average value was used as the representative value of the green view index for each location. This guideline is widely referred to by local authorities in Japan when planning and evaluating green spaces in urban areas. We added 54 new sites to the green view index for the entire downtown area of Sapporo and took photographs at 77 sites.

Photographs were taken in two to six directions at each point, depending on the road type, so that the camera was parallel to the ground. Regarding the shooting direction, for pedestrian roads and roads without a sidewalk, photographs were captured in two directions of travel (Figs. 2a, 2b). Intersections were captured in four directions, from the corner to the center of the intersection (Fig. 2c). T-junctions were captured in five directions, from the corner to the center of the junction and two directions on sidewalks and the opposite side (Fig. 2d). If there were sidewalks on both sides of the road, photographs were taken in two directions on both sidewalks and toward the sidewalk on the opposite side (Fig. 2e). A total of 350 photos were obtained. The green visibility at each point was the average of the green visibility of the photographs taken in multiple directions.

2.3. Google Street View (GSV)

In the GSV method, the latitude and longitude of the point to be acquired, the direction of the photograph, the angle of the horizontal field of view, the camera angle, and the output image size were set in the URL of the Street View Static API. The setting of the shooting position and direction of the photo were slightly different from that of the GSV in the field because the GSV was taken from the road. If there was a road without a sidewalk or a pedestrian road, there were two directions of travel (Figs. 3a, 3b). At intersections, photographs were taken from the center to the corner of intersection (Fig. 3c). At T-junctions, photographs were taken from the center to the three directions of travel and a direction perpendicular to the sidewalk (Fig. 3d). For a road with a sidewalk on both sides, there were two directions of travel on the road and two directions perpendicular to the sidewalk on both sides of the road (Fig. 3e). The horizontal viewing angle was set to 62°, the camera angle was set to 0° (i.e., horizontal), and the output image size was set to 480 × 360 pixels so that the aspect ratio was 4:3. We created a URL with parameters set for each photograph and acquired GSV photos via Git-Bash calling the Street View Static API. A total of 301 photos were obtained. The green visibility at each point was taken as the average of the green visibility of the photographs taken in multiple directions.

2.4. Calculation of Green View Index (GVI) and analysis

The automatic image identification AI used was DeepLab v3 Plus, developed by Google in 2018. We also used a pre-trained model called "xception65_cityscapes_trainfine," which was trained using the datasets "CityScapes train fine set" and "ImageNet." CityScapes specializes in the segmentation of urban streets and is widely used and reliable (Nagata et al., 2020). The DeepLab trained in this way can be used to identify, segment, and label elements of the following 20 types: road, sidewalk, person, rider, car, truck, bus, train, motorcycle, bicycle, building, wall, fence, pole, traffic sign, traffic light, vegetation, terrain, and sky. In addition, Python code running on a PC (Windows 10 Pro, 8 Gb RAM, Intel Core i5) was used to automate the process of loading the target photos, performing image segmentation analysis, and calculating the GVI.

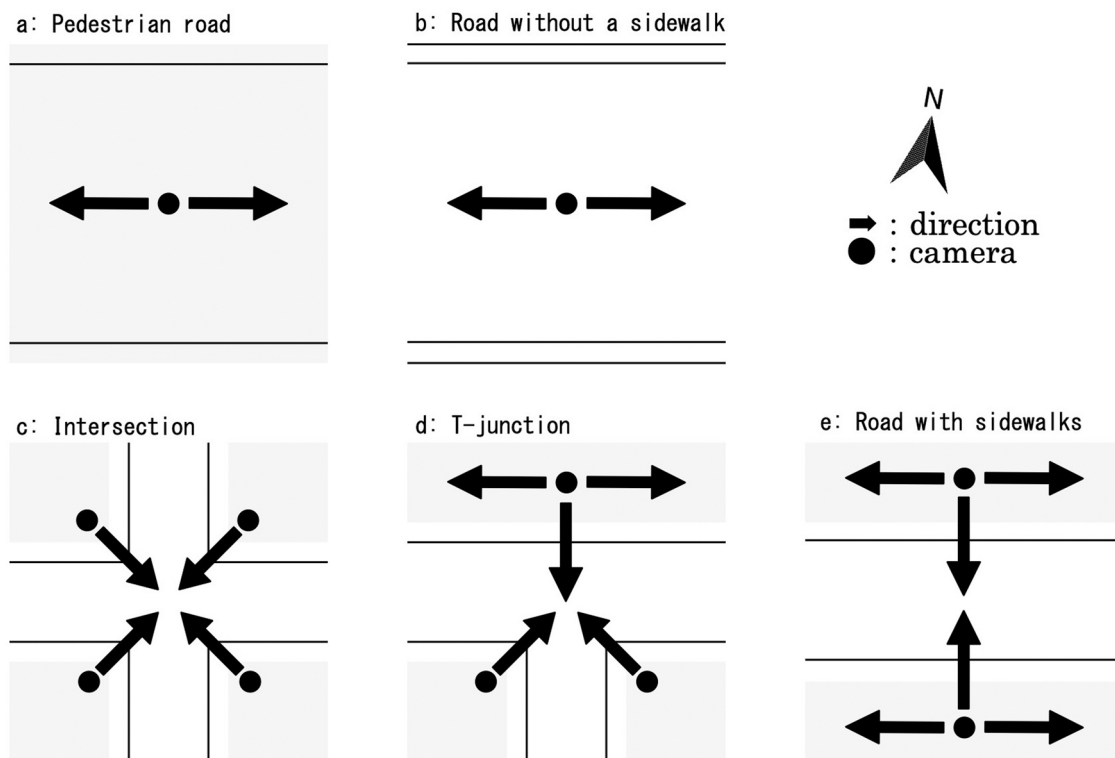


Fig. 2. Position and Direction for Photography.

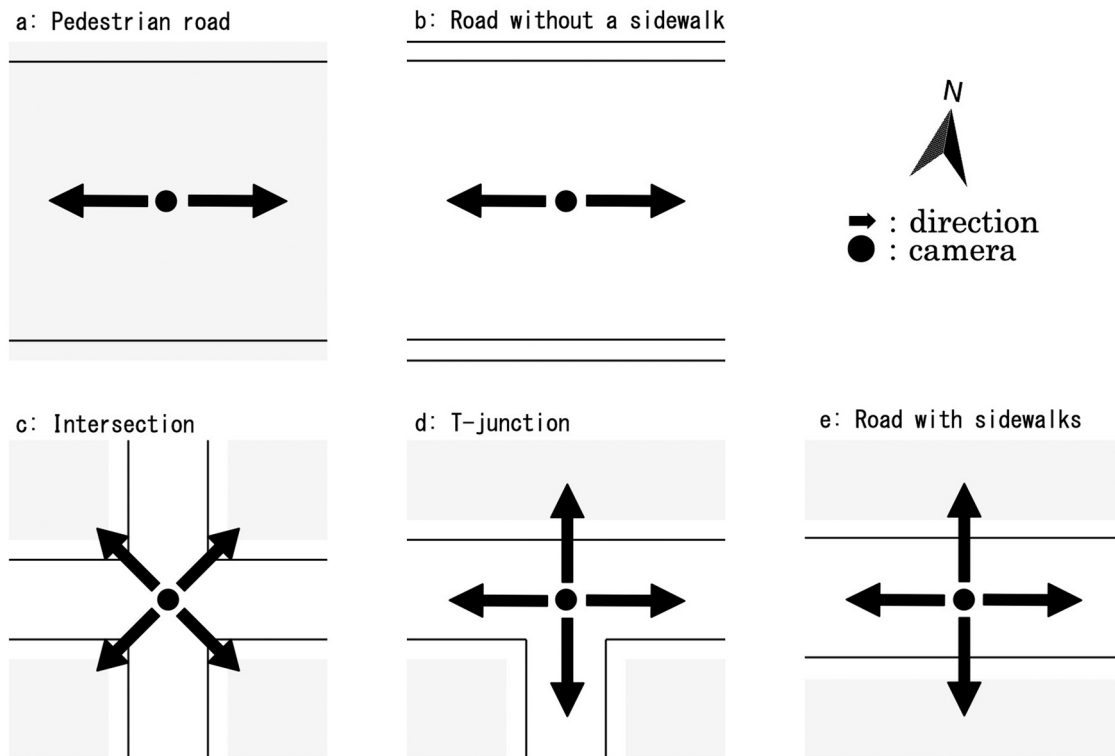


Fig. 3. Position and Direction for GSV.

We calculated the GVI of the on-site photographs taken in 2019 and gathered GSV photographs using DeepLab. Moreover, we calculated the GVI of 68 photographs taken by Sapporo City during the five days from the end of June to the end of July 2004 using DeepLab. The GVI was also calculated by a conditional method implemented by a trained graduate

student using Photoshop. Following some of the previous studies (Yang et al., 2009; Jiang et al., 2014; Labib et al., 2021), the photos were imported into Photoshop and the areas corresponding to vegetation such as tree trunks and leaves, were selected using the magic wand tool. Then, operators manually added leaves and branches outside of the range and

manually deleted selections that were not vegetation. The number of pixels in the selected area was counted and divided by the number of pixels in the entire photograph to calculate the GVI. The green visibility at each point was the average of the green visibility of the photographs taken in multiple directions. In addition, calculation time was recorded.

We then compared the GVI at each site using photos taken in the field and the GSV images. To clarify the characteristics of the GSV photo collection and image segmentation by DeepLab, photos with significant differences in the measured GVI were compared.

3. Results

3.1. GVI comparison between manual and automatic measurement

Fig. 4 shows a scatter plot and the regression analysis results of the GVI by DeepLab and Photoshop for 69 photographs taken in 2004 and

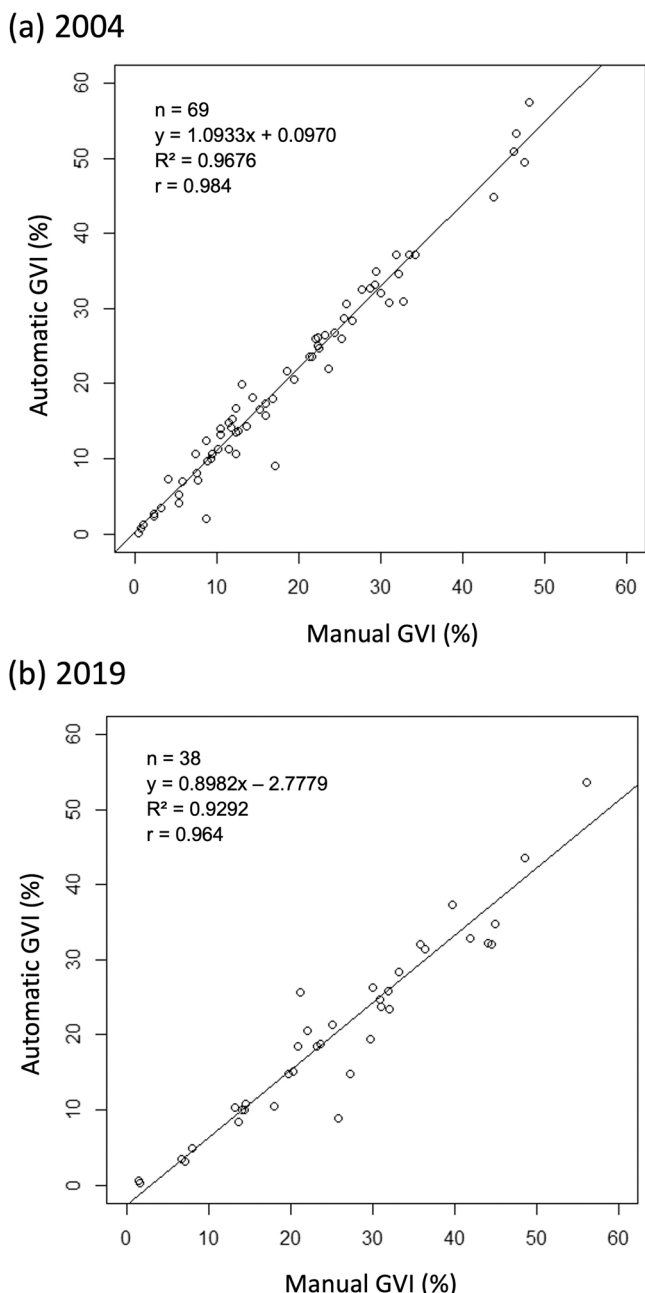


Fig. 4. Correlation of the GVI between Manual and Automatic Calculation.

38 in 2019. The correlation between the results using Photoshop and DeepLab was 0.984 ($p < 0.001$) for 69 photographs taken in 2004, and 0.964 ($p < 0.001$) for 38 photographs taken in 2019.

The difference in GVI between Photoshop and DeepLab ranged from – 8.09 to 9.44%. Of the 69 photos taken in 2004, 57 had a higher GVI when calculated by DeepLab versus using Photoshop, but 11 photos differed by less than 1%, 41 photos by 1–5%, and five photos by 5% or more. In contrast, there were 12 photos with a lower GVI according to DeepLab versus using Photoshop, of which 10 photos had a difference of less than 5%. For the photos taken in 2019, the difference was from – 16.99 to 4.54%. Of the 38 photographs, only one had greater GVI as calculated by DeepLab versus Photoshop. Of the 37 photographs with smaller GVI according to DeepLab versus Photoshop, 19 were 1–5% smaller, and 17 were 5% or more.

We confirmed that the GVI calculated by DeepLab generally exceeded that calculated using Photoshop. As shown in **Fig. 5**, the outline of trees identified as “vegetation” by DeepLab was often relatively rough. The branches without leaves were also comprehensively identified, and the green in the foreground and the background were continuously identified without any gaps. The images also contained relatively large trees. We then inspected the photo analysis results for those where the GVI was smaller as calculated by DeepLab versus Photoshop. As shown in **Fig. 6**, the lawn in the median strip was identified as “road.” Similarly, in some photographs, the flowers planted in the ground were identified as “fence”; the shrubs along the fence planting as “car,” “fence,” and “person”; the lawn as “fence”; and the distant green region as “building.”

It required a total of 1323 min (c. 22 h; 35 min average per image) to calculate the green visibility of all 38 photos using Photoshop. The longest duration was 107 min (GVI = 36.5%) and the shortest was 6 min (GVI = 1.7%). Many artificial objects, such as electric wires, poles, and fences, were covered with green, and it was time-consuming to identify fragmented vegetation. For 69 photos taken in 2004, the GVI was calculated for all images simultaneously using DeepLab, which required 3553 s (approximately 59 min), for an average of approximately 51 s per photograph. For 38 photographs taken in 2019, it required 1927 s (approximately 32 min), at approximately 51 s per photograph.

3.2. GVI comparison between on-site photographs and GSV

We compared the GVI of the 73 sites where photographs were taken. **Fig. 7** shows a scatterplot of the GVI at each site and the regression analysis results were calculated using photographs taken on-site and collected by GSV. The correlation between the GVI at each site calculated using the on-site photograph and the GSV photograph was 0.966 ($p < 0.001$). The difference between the results obtained on-site and from GSV ranged from – 9.0 to 13.0%. Of the 77 sites, 64 differed by less than $\pm 5\%$, and 29 differed by less than $\pm 1\%$. There were seven sites for which the GVI calculated from GSV was less than that calculated using on-site images. Conversely, there were three sites for which the GVI calculated from GSV was higher than that calculated using on-site images.

As shown in **Fig. 8**, some GSV photographs were taken when there were few leaves on the street trees. In addition, some vegetation was behind the cars on the street in the GSV photographs. There were also differences in the distance to the vegetation due to differences in the shooting position between the on-site and the GSV approaches. The on-site photographs were taken from the sidewalk, and the vegetation on the same sidewalk was shown clearly; green regions were close to the camera. In contrast, GSV captured the vegetation on the sidewalk from the road so that the distance between the camera and vegetation was larger. As shown in **Fig. 9**, the GVI calculated using GSV was larger than calculated using on-site photographs because it was more optimal to shoot from the center of the road. For example, there might be a tree at the corner of the district, or the district is part of a park. The distance to the trees was closer at such sites, and the amount of vegetation in the photos increased.

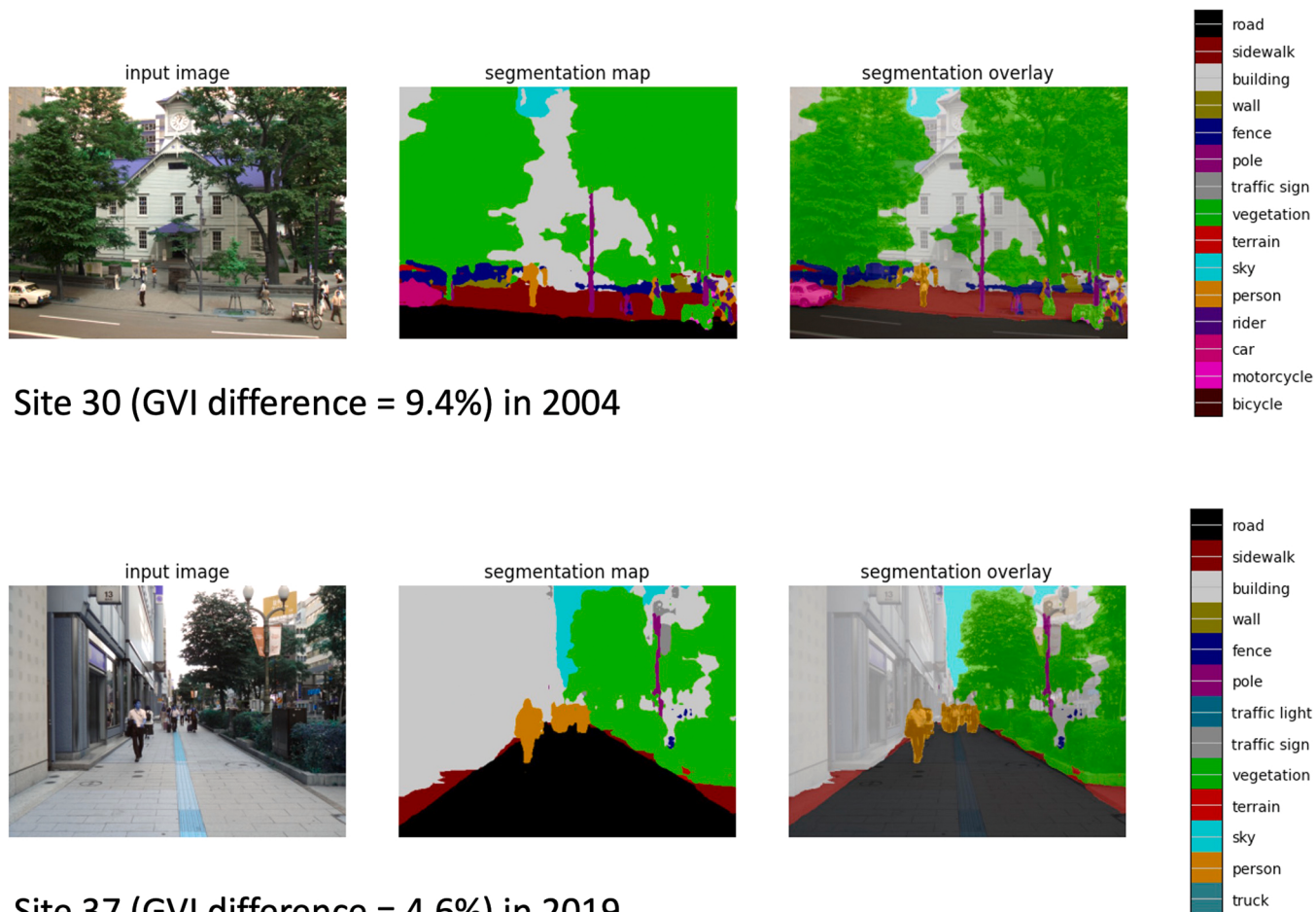


Fig. 5. Photographs for which the Automatic GVI was Larger than the Manual GVI.

The on-site shooting took nine days. To avoid backlighting, there were restrictions due to the weather, such as avoiding sunny days and not being able to shoot on rainy days. In contrast, in the GSV method, a URL with embedded parameters was defined, read via GitBash, and all GSV photos were collected simultaneously. It required approximately 5 min to obtain all 301 and 292 photographs at 73 sites.

4. Discussion

We compared the conventional method of calculating the GVI using image editing software and the modern method of using automatic image segmentation AI using photographs taken on-site in different years. The correlation between the GVI results using DeepLab and Photoshop was 0.97 for photographs taken in 2004 and 0.95 for photographs taken in 2019, indicating that the GVI calculations of DeepLab are comparable to manual calculations. Labib et al. (2021) mentioned that the manual Photoshop method is more accurate, but they did not provide specific evidence. Correlations between greenness calculations by some of these automatic image identification AIs and conventional Photoshop-based manual greenness calculations have been shown, such as $r = 0.91$ for PSPNet (Lu, 2018), $r = 0.899$ (Ye et al., 2019a) or 0.992 (Dong et al., 2018) or 0.98 (Zhang and Dong, 2018) for SegNet and $r = 0.90$ for FCN-8s (L. Yang et al., 2021), $r = 0.98$ for Back Propagation neural-network (Chen et al., 2019), $r = 0.9552$ for DeepLab (Xia et al., 2021). Among these, several studies have specifically shown scatter plots of GVI with manual methods and semantic segmentation (Dong et al., 2018; Zhang and Dong, 2018; Chen et al., 2019; Xia et al., 2021). The results of this study are similar, with the regression equation nearly

diagonal, the inclination of the regression line close to 1, and the intercept close to 0. It was shown that the measurement of GVI by machine learning produces results that approximate those of the manual method.

Automating the process allows many photos to be processed simultaneously, making it possible to conduct a large-scale survey with little effort. The identification of greenery on windows and green artificial objects can be an issue when calculating the GVI using color, as such regions may sometimes be incorrectly identified as "vegetation" (Lu, 2019; Tonosaki, 2010); however, the effect was almost negligible in the current study. Nevertheless, the models trained on the CityScapes and ImageNet datasets showed that greenery reflected in windows could also be misidentified. It was also found that some artificial objects, such as shadows of trees on the ground and stone blocks surrounding plantings, were sometimes identified as "vegetation." Even after considering these factors, the correlation between the results of the automated approach and those calculated using the image editing software remained high. Nagata et al. (2020) found the interaction effect between the road and the terrain segments or between the sidewalk and terrain segments by DeepLab. To further improve the accuracy, DeepLab needs to be trained to be closer to pedestrian perception.

DeepLab identified tree outlines roughly as vegetation, whereas the manual method identified leaves and branches in more detail. The operator visually recognizes and fills in vegetation and is affected minimally by the contrast or exposure of the image due to weather conditions. However, there are cases for which it is difficult to determine how finely to trace and fill in the outlines of trees, such as when the outlines of the leaves are complicated, when the greenery is achromatic

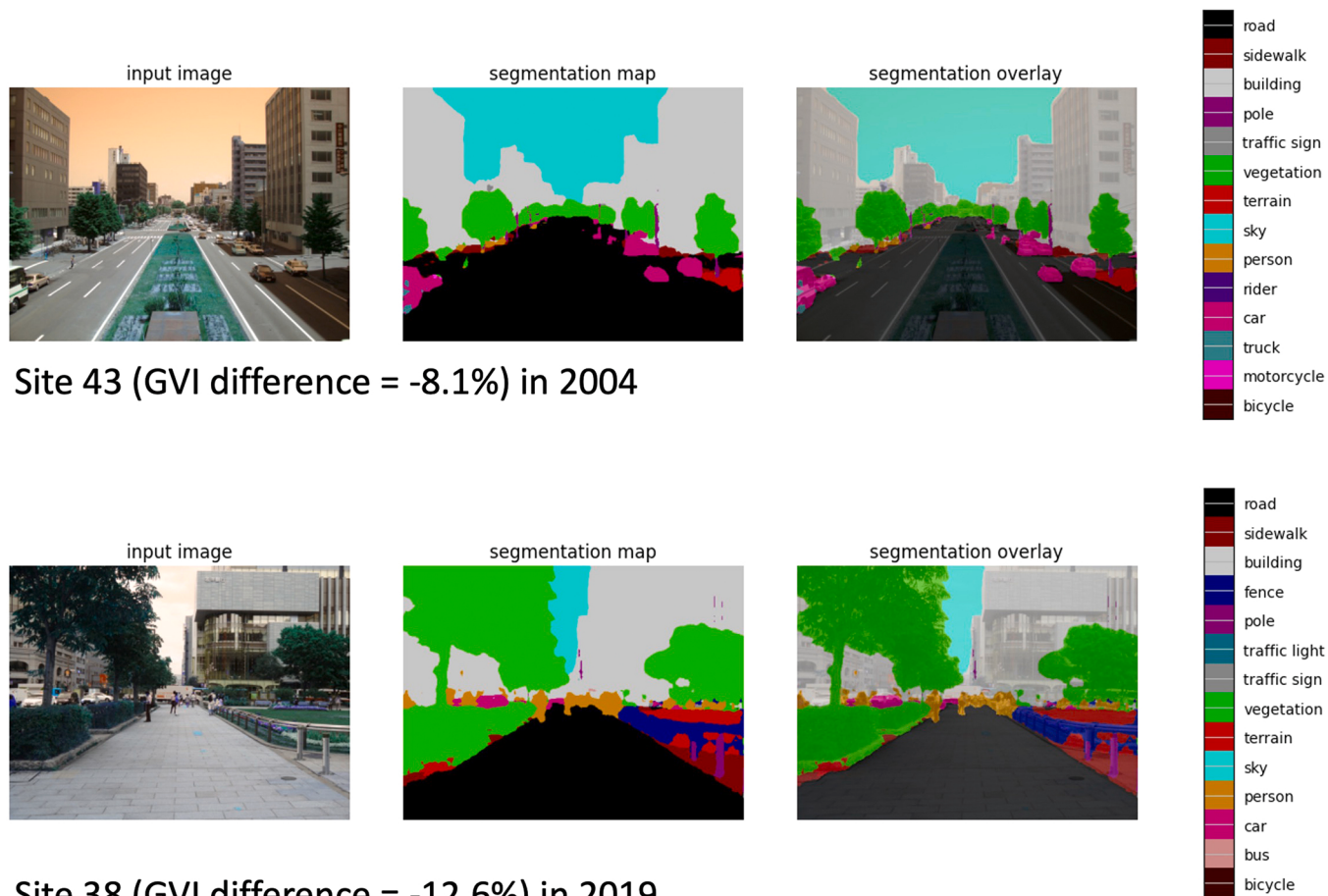


Fig. 6. Photographs for which the Automatic GVI was Smaller than the Manual GVI.

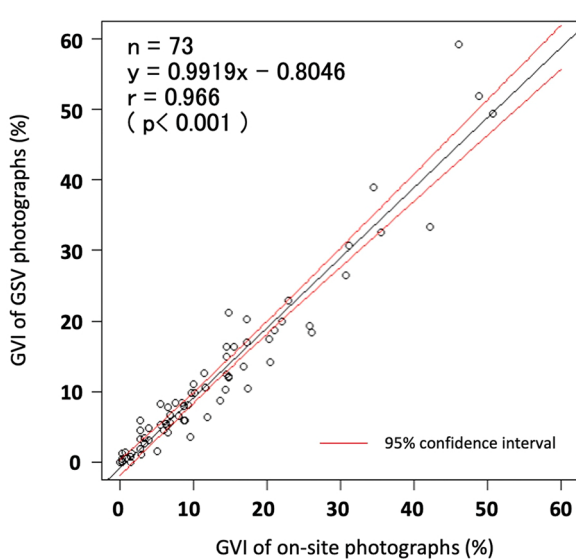


Fig. 7. Correlation of the GVI when Using On-site and GSV Photographs.

in the shade, when the greenery appears small in the distance, when weeds are distinguished from grass, and when the greenery is covered with artificial objects such as electric wires, poles, and fences. This indicates that the results, accuracy, and time required to extract greenery and calculate the greenness ratio using Photoshop may vary depending on the operator.

In terms of efficiency, we found that it required approximately 30 min on average to calculate the GVI per image using image editing software, which suggests a limit to the number of images that can be processed. In contrast, DeepLab required approximately 51 s per image. The implementation of DeepLab on a standard spec PC made it possible to analyze all photographs and calculate the GVIs simultaneously, regardless of the number of photos. Therefore, the time and effort required for the calculation was significantly reduced. Because image segmentation is based on pixel-by-pixel discrimination, the calculation time is related to the image size. The time required to calculate the greenery ratio for GSV photos of 480 × 360 pixels (25–50 Kb of data) was approximately 42 s per photo.

In contrast, the photographs taken in the field that required approximately 51 s to process were 4608 × 3456 pixels (1–4 Mb file size). Therefore, reducing the data size makes it possible to perform the calculation somewhat more quickly. The effect of resolution on the calculation time could be considered, but the resolution of the photographs taken on-site in 2004 and 2019 was 72 dpi, and that of the GSV photographs was 96 dpi. In this study, the resolution did not vary considerably, unlike the image size. The specification of the PC used in this study was not very high. That a high-specification PC is not needed will make it easier for planners and practitioners to conduct GVI surveys and incorporate them as environmental indicators.

A comparison was made between the conventional method of collecting photographs on-site and the modern method using GSV. The correlation between the GSV and on-site photographs was 0.966. Previous studies have noted some differences between GSV images and the human field of view on the sidewalk and various factors affecting the measurement of green view index, but no comparison between field



On-site photographs



GSV photographs

Site 26



On-site photographs



GSV photographs

Site 60

Fig. 8. Sites for which the GVI of GSV Photographs were Smaller than those of On-site Photographs.

On-site photographs



GSV photographs

Site 49

Fig. 9. Sites for which the GVI of GSV Photographs were Larger than that of On-site Photographs.

photographs and GSV has been made. In this study, the correlation between the photography method and the green view index calculation was high, the slope of the regression equation was close to 1, and the intercept was small. We confirmed that GSV approximates the green view index of field photography. The GSV approach is also excellent in terms of efficiency. For each photo, we set parameters such as latitude, longitude, and direction for each URL. Using Excel, Python, R, GitBash, and other tools as appropriate, we obtained many photographs at once. We found that the oldest GSVs were taken in 2010, and the latest GSVs were taken in 2019.

However, some problems remain to be solved. First, the distance between the GSV and the object, such as a sidewalk, differs depending on the direction, even at the same point because the GSV is a photograph taken while driving in one of several lanes. Therefore, there are cases for which the distance to the greenery is too far or too close. For this reason, it is necessary to check the obtained photos, especially when the survey point is on a wide road with many lanes. Next, the researcher could not define the season in which GSV photographs were obtained. It is possible to obtain photographs taken in winter (Lu, 2019), including leafless trees. Moreover, cars sometimes hide vegetation due to heavy traffic in the GSV photographs. Therefore, it was observed that the GVI of these GSV photos was sometimes lower than that of the on-site photographs.

Regarding the shooting conditions and settings of such photos, GSV photographs are taken from the roadway, so that they show greenery within the range of view of pedestrians, but not from the perspective of actual pedestrians. Therefore, the utility of the GSV images could be further verified by clarifying how differences in the photographer's viewpoint affect the GVI values. Consequently, it is also necessary to investigate GSV images and photographs taken in the field at the exact same location. A slight difference in GVI might affect pedestrians' preferences of city streets. The flowers beneath trees which might be hidden in the GSV, are the most preferred element on city streets (Todorova et al., 2004). The amount of greenery and its preference are related to the power trend line (Jiang et al., 2015; Suppakittpaisarn et al., 2019). A small increase in low-density greenery may greatly increase its preference. When considering the GVI calculated by automatic methods using GSV, such slight differences cannot be ignored.

GSV does not necessarily produce photographs that are the same as those taken in the field. However, the correlation between GSV and conventional methods and the high efficiency of GSV show that it is an effective alternative to field photography. The use of GSV for photo collection will enable planners and practitioners to conduct various studies and surveys more efficiently and quickly, using green coverage on a large scale.

There is some need for further research; GSV photos were shown to differ from those taken on the sidewalk. Some studies have utilized panoramic photographs and 3-D Video as a measure of greenness, to approximate the pedestrian experience (Jiang et al., 2014; Jiang et al., 2015; Jiang et al., 2016; Gong et al., 2018). More work needs to be done on the medium of assessment of green view index. In addition, this study only compared GVI by Photoshop and GVI by DeepLab. Additional verification is needed to determine whether the GVI calculated by these methods actually differs from the human perception of greenness, referring to previous studies. Furthermore, in the present study, the resolution of the GSV photographs was different from that of the photographs taken in the field, and it is necessary to verify to what extent the differences in the size and resolution of the photographs affect the GVI in deciphering the photographs using Photoshop.

5. Conclusion

In this study, we focused on the GVI, which has been attracting attention as an indicator of greenness in recent years and attempted to improve the efficiency of the measurement method, which has been a problem. We found that using GSV to collect photos and automatic image identification AI to calculate the GVI of the obtained photos

significantly reduced the time and labor demands and was effective as an alternative method.

One of the problems with GSV is that it is impossible to specify the time of day, so that photographs may have been taken when there were few leaves or when cars are present. In addition, due to the variable widths of the driving lanes in which the GSV photography cars were traveling, the distance from greenery in the images varied greatly for the same location, which had a significant impact on the GVI.

We used the CityScapes dataset for the automatic image segmentation AI. The dataset specializes in urban landscapes and has been widely used for automatic driving applications. However, we found that the dataset was inferior for identifying grasses, ground cover plants, and flowers. Therefore, it would be helpful to develop or train datasets in the future. Models specialized for vegetation identification, such as those that can divide vegetation into different types such as "trees," "shrubs," "flowers," "lawns," and "wall greening." This would also be of utility for research related to the quality of greenery. Further research and technological development may improve the accuracy of the GSV and the automatic image segmentation AI approaches.

CRediT authorship contribution statement

Tetsuya Aikoh: Conceptualization, Project administration, Writing – original draft, Writing – review & editing. **Riko Homma:** Visualization, Data curation, Formal analysis, Writing – original draft. **Yoshiki Abe:** Data curation, Software, Investigation, Writing – review & editing.

Declaration of Competing Interest

The authors declare that they have no known competing financial interests or personal relationships that could have appeared to influence the work reported in this paper.

Acknowledgments

The authors would like to thank the Sapporo City Greenery Promotion Department for sharing the photographs and datasets on green view index.

References

- Aoki, Y., 1991. Evaluation methods for landscapes with greenery. *Landsc. Res.* 16 (3), 3–6.
- Badrinarayanan, V., Kendall, A., Cipolla, R., 2017. Segnet: a deep convolutional encoder-decoder architecture for image segmentation. *IEEE Trans. Pattern Anal. Mach. Intell.* 39 (12), 2481–2495.
- Berland, A., Lange, D.A., 2017. Google street view shows promise for virtual street tree surveys. *Urban For. Urban Green.* 21, 11–15.
- Beyer, K.M., Kaltenbach, A., Szabo, A., Bogar, S., Nieto, F.J., Malecki, K.M., 2014. Exposure to neighborhood green space and mental health: evidence from the survey of the health of Wisconsin. *Int. J. Environ. Res. Public Health* 11 (3), 3453–3472.
- Bjerke, T., Østdahl, T., Thrane, C., Strumse, E., 2006. Vegetation density of urban parks and perceived appropriateness for recreation. *Urban For. Urban Green.* 5 (1), 35–44.
- Browning, M.H., Lee, K., Wolf, K.L., 2019. Tree cover shows an inverse relationship with depressive symptoms in elderly residents living in US nursing homes. *Urban For. Urban Green.* 41, 23–32.
- Buxton, J.A., Ryan, R.L., Wells PhD, N.M., 2019. Exploring preferences for urban greening. *Cities Environ. (CATE)* 12 (1), 3.
- Chen, X., Meng, Q., Hu, D., Zhang, L., Yang, J., 2019. Evaluating greenery around streets using Baidu panoramic street view images and the panoramic green view index. *Forests* 10 (12), 1109.
- Chen, X.L., Zhao, H.M., Li, P.X., Yin, Z.Y., 2006. Remote sensing image-based analysis of the relationship between urban heat island and land use/cover changes. *Remote Sens. Environ.* 104 (2), 133–146.
- Chen, L.C., Zhu, Y., Papandreou, G., Schroff, F., & Adam, H. (2018). Encoder-decoder with atrous separable convolution for semantic image segmentation. In *Proceedings of the European Conference on Computer Vision (ECCV)* (pp. 801–818).
- Chen, J., Zhou, C., Li, F., 2020. Quantifying the green view indicator for assessing urban greening quality: An analysis based on Internet-crawling street view data. *Ecol. Indic.* 113, 106192.
- Chen, Z., Xu, B., Gao, B., 2015. Assessing visual green effects of individual urban trees using airborne Lidar data. *Sci. Total Environ.* 536, 232–244.

- Cohen-Cline, H., Turkheimer, E., Duncan, G.E., 2015. Access to green space, physical activity and mental health: a twin study. *J. Epidemiol. Community Health* 69 (6), 523–529.
- Derkzen, M.L., van Teeffelen, A.J., Verburg, P.H., 2015. Quantifying urban ecosystem services based on high-resolution data of urban green space: an assessment for Rotterdam, the Netherlands. *J. Appl. Ecol.* 52 (4), 1020–1032.
- Dong, R., Zhang, Y., Zhao, J., 2018. How green are the streets within the sixth ring road of Beijing? An analysis based on Tencent Street View pictures and the green view index. *Int. J. Environ. Res. Public Health* 15 (7), 1367.
- Douglas, O., Lennon, M., Scott, M., 2017. Green space benefits for health and well-being: A life-course approach for urban planning, design and management. *Cities* 66, 53–62.
- Dwyer, J.F., Schroeder, H.W., Gobster, P.H., 1991. The significance of urban trees and forests: toward a deeper understanding of values. *J. Arboric.* 17 (10), 276–284.
- Dymond, J.R., Stephens, P.R., Newsome, P.F., Wilde, R.H., 1992. Percentage vegetation cover of a degrading rangeland from SPOT. *Int. J. Remote Sens.* 13 (11), 1999–2007.
- Elsadek, M., Liu, B., Lian, Z., Xie, J., 2019. The influence of urban roadside trees and their physical environment on stress relief measures: A field experiment in Shanghai. *Urban For. Urban Green.* 42, 51–60.
- Falfán, I., Muñoz-Robles, C.A., Bonilla-Moheno, M., MacGregor-Fors, I., 2018. Can you really see 'green'? Assessing physical and self-reported measurements of urban greenery. *Urban For. Urban Green.* 36, 13–21.
- Gao, X., Asami, Y., 2007. Effect of urban landscapes on land prices in two Japanese cities. *Landscape. Urban Plan.* 81 (1–2), 155–166.
- Garcia-Garcia, A., Orts-Escolano, S., Oprea, S., Villena-Martinez, V., Martinez-Gonzalez, P., Garcia-Rodriguez, J., 2018. A survey on deep learning techniques for image and video semantic segmentation. *Appl. Soft Comput.* 70, 41–65.
- Gong, F.Y., Zeng, Z.C., Zhang, F., Li, X., Ng, E., Norford, L.K., 2018. Mapping sky, tree, and building view factors of street canyons in a high-density urban environment. *Build. Environ.* 134, 155–167.
- Griew, P., Hillsdon, M., Foster, C., Coombes, E., Jones, A., Wilkinson, P., 2013. Developing and testing a street audit tool using Google Street View to measure environmental supportiveness for physical activity. *Int. J. Behav. Nutr. Phys. Act.* 10 (1), 1–7.
- Gupta, K., Kumar, P., Pathan, S.K., Sharma, K.P., 2012. Urban neighborhood green index—a measure of green spaces in urban areas. *Landscape. Urban Plan.* 105 (3), 325–335.
- Holtan, M.T., Dieterlen, S.L., Sullivan, W.C., 2015. Social life under cover: tree canopy and social capital in Baltimore, Maryland. *Environ. Behav.* 47 (5), 502–525.
- Jiang, B., Chang, C.Y., Sullivan, W.C., 2014. A dose of nature: Tree cover, stress reduction, and gender differences. *Landscape. Urban Plan.* 132, 26–36.
- Jiang, B., Larsen, L., Deal, B., Sullivan, W.C., 2015. A dose-response curve describing the relationship between tree cover density and landscape preference. *Landscape. Urban Plan.* 139, 16–25.
- Jiang, B., Li, D., Larsen, L., Sullivan, W.C., 2016. A dose-response curve describing the relationship between urban tree cover density and self-reported stress recovery. *Environ. Behav.* 48 (4), 607–629.
- Jiang, B., Deal, B., Pan, H., Larsen, L., Hsieh, C.H., Chang, C.Y., Sullivan, W.C., 2017. Remotely-sensed imagery vs. eye-level photography: Evaluating associations among measurements of tree cover density. *Landscape. Urban Plan.* 157, 270–281.
- Jin, C.Y., Chen, W.Y., 2008. Assessing the ecosystem service of air pollutant removal by urban trees in Guangzhou (China). *J. Environ. Manag.* 88 (4), 665–676.
- Ki, D., Lee, S., 2021. Analyzing the effects of Green View Index of neighborhood streets on walking time using Google Street View and deep learning. *Landscape. Urban Plan.* 205, 103920.
- Kumakoshi, Y., Chan, S.Y., Koizumi, H., Li, X., Yoshimura, Y., 2020. Standardized green view index and quantification of different metrics of urban green vegetation. *Sustainability* 12 (18), 7434.
- Labib, S.M., Huck, J.J., Lindley, S., 2021. Modelling and mapping eye-level greenness visibility exposure using multi-source data at high spatial resolutions. *Sci. Total Environ.* 755, 143050.
- Lee, A.C., Maheswaran, R., 2011. The health benefits of urban green spaces: a review of the evidence. *J. Public Health* 33 (2), 212–222.
- Leslie, E., Sugiyama, T., Ierodiakonou, D., Kremer, P., 2010. Perceived and objectively measured greenness of neighbourhoods: Are they measuring the same thing? *Landscape. Urban Plan.* 95 (1–2), 28–33.
- Li, D., Deal, B., Zhou, X., Slavenas, M., Sullivan, W.C., 2018. Moving beyond the neighborhood: daily exposure to nature and adolescents' mood. *Landscape. Urban Plan.* 173, 33–43.
- Li, X., Zhang, C., Li, W., Ricard, R., Meng, Q., Zhang, W., 2015a. Assessing street-level urban greenery using Google Street View and a modified green view index. *Urban For. Urban Green.* 14 (3), 675–685.
- Li, X., Zhang, C., Li, W., Kuzovkina, Y.A., Weiner, D., 2015b. Who lives in greener neighborhoods? The distribution of street greenery and its association with residents' socioeconomic conditions in Hartford, Connecticut, USA. *Urban For. Urban Green.* 14 (4), 751–759.
- Li, X., Ratti, C., Seiferling, I., 2017. Mapping Urban Landscapes Along Streets Using Google Street View. In: Peterson, M. (Ed.), *Advances in Cartography and GIScience. ICACI 2017. Lecture Notes in Geoinformation and Cartography*. Springer, Cham. https://doi.org/10.1007/978-3-319-57336-6_24.
- Liu, W., Chen, W., Peng, C., 2014. Assessing the effectiveness of green infrastructures on urban flooding reduction: A community scale study. *Ecol. Model.* 291, 6–14.
- Liu, Y., Xiao, T., Liu, Y., Yao, Y., Wang, R., 2021. Natural outdoor environments and subjective well-being in Guangzhou. In: *Urban Forestry & Urban Greening*, 59. Comparing different measures of access, China, 127027.
- Long, Y., Liu, L., 2017. How green are the streets? An analysis for central areas of Chinese cities using Tencent Street View. *PLoS One* 12 (2), e0171110.
- Lu, Y., 2018. The association of urban greenness and walking behavior: Using Google Street View and deep learning techniques to estimate residents' exposure to urban greenness. *Int. J. Environ. Res. Public Health* 15 (8), 1576.
- Lu, Y., Sarkar, C., Xiao, Y., 2018. The effect of street-level greenery on walking behavior: Evidence from Hong Kong. *Soc. Sci. Med.* 208, 41–49.
- Lu, Y., 2019. Using Google Street View to investigate the association between street greenery and physical activity. *Landscape. Urban Plan.* 191, 103435.
- Nagata, S., Nakaya, T., Hanibuchi, T., Amagasa, S., Kikuchi, H., Inoue, S., 2020. Objective scoring of streetscape walkability related to leisure walking: statistical modeling approach with semantic segmentation of Google Street View images. *Health Place* 66, 102428.
- Nowak, D.J., Crane, D.E., 2002. Carbon storage and sequestration by urban trees in the USA. *Environ. Pollut.* 116 (3), 381–389.
- Odgers, C.L., Caspi, A., Bates, C.J., Sampson, R.J., Moffitt, T.E., 2012. Systematic social observation of children's neighborhoods using Google Street View: a reliable and cost-effective method. *J. Child Psychol. Psychiatry* 53 (10), 1009–1017.
- Onishi, A., Cao, X., Ito, T., Shi, F., Imura, H., 2010. Evaluating the potential for urban heat-island mitigation by greening parking lots. *Urban For. Urban Green.* 9 (4), 323–332.
- Osaka Prefecture (2013). *Green View Index Survey Guideline*, Osaka Prefecture.
- Poursaeed, O., Matera, T., Belongie, S., 2018. Vision-based real estate price estimation. *Mach. Vis. Appl.* 29 (4), 667–676.
- Rundle, A.G., Bader, M.D., Richards, C.A., Neckerman, K.M., Teitler, J.O., 2011. Using Google Street View to audit neighborhood environments. *Am. J. Prev. Med.* 40 (1), 94–100.
- Schroeder, H.W., Cannon, W.N., 1983. The esthetic contribution of trees to residential streets in Ohio towns. *J. Arboric.* 9 (9), 237–243.
- Seiferling, I., Naik, N., Ratti, C., Proulx, R., 2017. Green streets—quantifying and mapping urban trees with street-level imagery and computer vision. *Landscape. Urban Plan.* 165, 93–101.
- Soga, M., Evans, M.J., Tsuchiya, K., Fukano, Y., 2021. A room with a green view: the importance of nearby nature for mental health during the COVID-19 pandemic. *Ecol. Appl.* 31 (2), e2248.
- Suppakittpaisarn, P., Jiang, B., Slavenas, M., Sullivan, W.C., 2019. Does density of green infrastructure predict preference? *Urban For. Urban Green.* 40, 236–244.
- Suppakittpaisarn, P., Chang, C.Y., Deal, B., Larsen, L., Sullivan, W.C., 2020. Does vegetation density and perceptions predict green stormwater infrastructure preference? *Urban For. Urban Green.* 55, 126842.
- Suppakittpaisarn, P., Lu, Y., Jiang, B., Slavenas, M., 2022. How do computers see landscapes? comparisons of eye-level greenery assessments between computer and human perceptions. *Landscape. Urban Plan.* 227, 104547.
- Thayer, R.L., Atwood, B.G., 1978. Plants, complexity, and pleasure in urban and suburban environments. *Environ. Psychol. Nonverbal Behav.* 3 (2), 67–76.
- Todorova, A., Asakawa, S., Aikoh, T., 2004. Preferences for and attitudes towards street flowers and trees in Sapporo, Japan. *Landscape. Urban Plan.* 69 (4), 403–416.
- Tonosaki, K., 2010. Research on the new measurement method of the ratio of vertical green coverage with leaf colors. *Landscape. Res. Jpn. Online* 3, 26–31.
- Troy, A., Grove, J.M., O'Neil-Dunne, J., 2012. The relationship between tree canopy and crime rates across an urban-rural gradient in the greater Baltimore region. *Landscape. Urban Plan.* 106 (3), 262–270.
- Tyrväinen, L., Ojala, A., Korpela, K., Lanki, T., Tsunetsugu, Y., Kagawa, T., 2014. The influence of urban green environments on stress relief measures: A field experiment. *J. Environ. Psychol.* 38, 1–9.
- Wolf, K.L., 2005. Business district streetscapes, trees, and consumer response. *J. For.* 103 (8), 396–400.
- Wu, J., Wang, B., Ta, N., Zhou, K., Chai, Y., 2020. Does street greenery always promote active travel? Evidence from Beijing. *Urban For. Urban Green.* 56, 126886.
- Xia, Y., Yabuki, N., Fukuda, T., 2021. Sky view factor estimation from street view images based on semantic segmentation. *Urban Clim.* 40, 100999.
- Xiao, Y., Miao, S., Zhang, Y., Chen, H., Wenjie, W.U., 2021. Exploring the health effects of neighborhood greenness on Lilong residents in Shanghai. *Urban For. Urban Green.* 66, 127383.
- Yang, J., Zhao, L., McBride, J., Gong, P., 2009. Can you see green? Assessing the visibility of urban forests in cities. *Landscape. Urban Plan.* 91 (2), 97–104.
- Yang, J., Rong, H., Kang, Y., Zhang, F., Chegut, A., 2021. The financial impact of street-level greenery on New York commercial buildings. *Landscape. Urban Plan.* 214, 104162.
- Yang, L., Liu, J., Liang, Y., Lu, Y., Yang, H., 2021. Spatially varying effects of street greenery on walking time of older adults. *ISPRS Int. J. Geo-Inf.* 10 (9), 596.
- Yang, Y., He, D., Gou, Z., Wang, R., Liu, Y., Lu, Y., 2019. Association between street greenery and walking behavior in older adults in Hong Kong. *Sustain. Cities Soc.* 51, 101747.
- Yang, Y., Lu, Y., Yang, H., Yang, L., Gou, Z., 2021. Impact of the quality and quantity of eye-level greenery on park usage. *Urban For. Urban Green.* 60, 127061.
- Ye, Y., Richards, D., Lu, Y., Song, X., Zhuang, Y., Zeng, W., Zhong, T., 2019a. Measuring daily accessed street greenery: A human-scale approach for informing better urban planning practices. *Landscape. Urban Plan.* 191, 103434.
- Ye, Y., Xie, H., Fang, J., Jiang, H., Wang, D., 2019b. Daily accessed street greenery and housing price: Measuring economic performance of human-scale streetscapes via new urban data. *Sustainability* 11 (6), 1741.
- Yin, L., Wang, Z., 2016. Measuring visual enclosure for street walkability: Using machine learning algorithms and Google Street View imagery. *Appl. Geogr.* 76, 147–153.

- Zhang, B., Xie, G., Zhang, C., Zhang, J., 2012. The economic benefits of rainwater-runoff reduction by urban green spaces: A case study in Beijing, China. *J. Environ. Manag.* 100, 65–71.
- Zhang, Y., Dong, R., 2018. Impacts of street-visible greenery on housing prices: Evidence from a hedonic price model and a massive street view image dataset in Beijing. *ISPRS Int. J. Geo-Inf.* 7 (3), 104.
- Zhou, H., He, S., Cai, Y., Wang, M., Su, S., 2019. Social inequalities in neighborhood visual walkability: Using street view imagery and deep learning technologies to facilitate healthy city planning. *Sustain. Cities Soc.* 50, 101605.